

# A Processor to get UV-B and UV-A Radiation Products in/from the ECMWF IFS

Jean-Jacques Morcrette, Antti Arola\*

Research Department

ECMWF, Shinfield Park, Reading  
RG2 9AX, United Kingdom

\*Finnish Met. Institute  
Kuopio, Finland

Jean-Jacques.Morcrette@ecmwf.int

June 27, 2007

*This paper has not been published and should be regarded as an Internal Report from ECMWF.  
Permission to quote from it should be obtained from the ECMWF.*



European Centre for Medium-Range Weather Forecasts  
Europäisches Zentrum für mittelfristige Wettervorhersage  
Centre européen pour les prévisions météorologiques à moyen terme

Series: ECMWF Technical Memoranda

A full list of ECMWF Publications can be found on our web site under:

<http://www.ecmwf.int/publications/>

Contact: [library@ecmwf.int](mailto:library@ecmwf.int)

©Copyright 2007

European Centre for Medium-Range Weather Forecasts  
Shinfield Park, Reading, RG2 9AX, England

Literary and scientific copyrights belong to ECMWF and are reserved in all countries. This publication is not to be reprinted or translated in whole or in part without the written permission of the Director. Appropriate non-commercial use will normally be granted under the condition that reference is made to ECMWF.

The information within this publication is given in good faith and considered to be true, but ECMWF accepts no liability for error, omission and for loss or damage arising from its use.

### Abstract

A new processor for evaluating the UV-B and UV-A radiation at the surface, based on modifications to the shortwave radiation scheme of the ECMWF IFS is described. First, sensitivity studies of the UV surface irradiance and Erythemal Dose Rate to the spectral resolution, to the representation and atmospheric contents of ozone and aerosol, and to the surface albedo are performed. Comparison of model UV with surface observations and the impact on UV surface flux of some recent ozone minima are used to illustrate the potential usefulness of the UV processor.

## 1. Introduction.

As part of the calculations of the physical tendencies in the ECMWF forecast model, the shortwave radiation transfer (SWRT) scheme (Fouquart and Bonnel, 1980; Morcrette, 2002) evaluates the ultra-violet (UV) fluxes over two spectral intervals (185 - 250 - 440 nm). The flux in the second interval is post-processed and archived as "UV-B", but at present is of very little use as the ozone entering the radiation transfer calculations is not the prognostic ozone, but the monthly climatological ozone from Fortuin and Langematz (1994). Accordingly, this UV-B flux displays the effects of clouds and climatological aerosols but is insensitive to variations in the prognostic ozone. Even if prognostic ozone were used as input, the averaging over such a wide spectral interval would make this flux hardly sensitive to ozone.

Seen from the surface, the ozone in the stratosphere absorbs all of the incoming UV-C ( $\lambda < 280$  nm), some of the shorter UV-B ( $280 < \lambda < 325$  nm) and very little of the UV-A ( $325 < \lambda < 400$  nm). In this respect, the UV community is interested in spectrally detailed information, from which a number of parameters (UV Index or erythemal action spectra, plant action spectra, DNA action spectra or biologically effective dose, erythemal local-noon irradiance) can be derived (For more detailed information, see <http://imk-ifu.fzk.de/photonics/actionspectrum.html>). Both an excess and a deficit in available UV-B at the surface are of concern with additional cancer and osteoporotic fractures being linked to excess UV irradiation, but vitamin D insufficiency being linked to deficit in UV-B availability (Grant et al., 2005).

Since the mid-90s, some of the above parameters are available, usually via a somewhat simplified processing of outputs from operational Numerical Weather Prediction (NWP) models, with Canada (Burrows et al., 1994), the US National Weather Service (Long et al., 1996) and the Australia Bureau of Meteorology (Lemus-Deschamps and Rikus, 1999) the first major centres to provide UV products. An intercomparison of the original methods used to diagnose UV at the surface is available in Koepke et al. (1998). A more recent survey can be found in Taalas et al. (2000).

As discussed by Long (2003), following some efforts from WMO aiming at standardising UV products (WMO, 1997), as of 2003, 30 countries were producing some UV Index information from meteorological models. The UV Index (UVI) is defined as the scaled integral of spectral irradiances between 290 and 400 nm weighted by the CIE (French for International Commission on Illumination) erythemal action spectrum (McKinlay and Diffey, 1987). The CIE action spectrum seeks to replicate the average human skin response to UV irradiances, with the largest sensitivity in that part of the UV spectrum (300 - 325 nm) which shows the greatest variability due to ozone changes and lesser sensitivity to the part of the UV spectrum ( $> 325$  nm) that varies the least with ozone changes. Convoluting the irradiances between 280 and 400 nm with the CIE action spectrum results in an erythemal dose rate (EDR) or Biologically Effective Dose (BED) (in units of  $Wm^{-2}$ ). The UVI is then determined by multiplying the EDR by  $40 (Wm^{-2})^{-1}$  resulting in a unitless value ranging from zero (at night) to greater than 15 on top of high mountains in the tropics at solar noon. The greater (lesser) the UVI, the shorter (longer) the period of time before skin damage will occur. Just how long the time of exposure can be depends upon various genetic factors, in particular the melanin content of the skin. Long (2003) also discusses the various approaches to the UV radiative transfer (RT), from spectrally detailed radiation schemes explicitly dealing with scattering and absorption to statistical relationships based on past UV measurements and applied to similar conditions of insolation, snow cover, vertically integrated amount of ozone, and cloud cover.

Conservative scattering generally prevails in clouds in the UV part of the spectrum (in absence of aerosols). Therefore, clouds have less impact in the UV than on the global radiation. This usually has led to a simplified treatment of cloud effects in UV schemes. Even with the more physically-based approach involving RT schemes run on outputs of meteorological forecast models, clouds are introduced at best as one equivalent cloudy layer, with effective cover and optical thickness (Mayer, 2005) or through a reduction factor relating clear-sky and total sky fluxes over the whole SW spectrum and in the UV (Bordewijk et al., 1995; Josefsson and Landelius,

2000). Such methods provide a quantitatively good estimation of the UV radiation at the surface, but no vertical information on, for example, the distribution of the UV heating rate. A few studies have accounted for the full cloudy RT, but usually outside an operational environment (Erlick et al., 1998). Aerosols may have a large effect on the UV RT in polluted areas, in condition of forest fires, biomass burning or desert dust. Attenuation is linked to their optical depth, but in presence of clouds, this effect is usually increased through the resulting non-conservative scattering of the mix of cloud particles and aerosols.

As part of GEMS (Global Environmental Monitoring System) Reactive Gases subproject 3, the UV-B and UV-A radiation (the radiation in the 280 to 325 nm and 325 to 400 nm ranges) is to be processed at high resolution (0.05 nm) using dedicated radiation transfer (RT) codes on outputs of the ECMWF Integrated Forecast System (IFS). Unfortunately, such RT codes are only able to deal with clear-sky and/or a one-layer cloudy sky. Work is therefore required to define from the ECMWF model cloud fraction and cloud ice and liquid water profiles such an equivalent cloud to be used in the detailed RT code.

This note describes an alternate/complementary approach, in which a new post-processor is applied to the ECMWF forecast fields, including prognosed ozone, and cloud fraction and water loading. This post-processor is based on the current SWRT scheme (cy29r2) and therefore handles clouds in a way consistent with the rest of the model physics. It includes more spectrally detailed descriptions (with either a 0.04, 0.2, 1 or 5 nm resolution) for the incident solar radiation at the top of the atmosphere (TOA), Rayleigh scattering, ozone absorption, aerosol and cloud scattering and absorption, and the surface albedo. It also uses the prognostic ozone, and, with its high spectral resolution, computes radiation quantities directly relevant for use by the UV community. It is thought that, by being fully consistent with the treatment of clouds but more spectrally detailed than the operational SWRT scheme, the outputs of this scheme could either be directly processed into parameters of interest for UV studies or provide insight for developing parametrisation of cloud effects for more benchmark RT codes.

In the future, the assimilation of aerosol-sensitive parameters in the analysis and the development of prognostic aerosols in the ECMWF IFS (Morcrette et al., 2005), as part of GEMS-Aerosol, should also improve the realism of the modelled UV fluxes at the surface.

Modifications to the shortwave radiation scheme are described in Section 2. Results from sensitivity to various input parameters are discussed in Section 3. Comparisons with UV surface observations carried out in some European stations are presented in Section 4. The impact on the UV surface fluxes of recent minima in ozone is shown as an illustration of the potential use of the UV processor in section 5. Perspectives are briefly discussed in section 6.

## 2. Methodology.

### *a. Is RT at spectral UV wavelengths different from broadband shortwave RT?*

Intrinsically, there are no differences between a spectrally defined radiative transfer at UV, visible or near-infrared wavelengths. The energy source is the Sun, its collimated radiation enters the atmosphere where it is scattered and absorbed going down in the atmosphere, and the resulting direct and diffuse radiation is further scattered and absorbed by gas molecules (Rayleigh scattering, absorption by the radiative active gases), cloud and aerosol particles (absorption and scattering) and the surface (absorption and reflection). A discussion on how the various atmospheric constituents contribute to the UV radiation at the surface can be found in Rikus (1997).

The difficulties stem from the less complete knowledge of the governing parameters in the RT in the UV than in the rest of the solar spectrum, and from the large variations occurring in the amplitudes of Rayleigh scattering,

solar spectral energy, and ozone absorption over this range of wavelength ( $\lambda$ ). Rayleigh scattering, varying as  $\lambda^{-4}$ , is obviously more intense for the shorter wavelengths, and similarly the phase function of any scattering medium (aerosol, clouds) is likely to be more peaked in the forward scattering direction at UV than at visible wavelengths. Particular attention is therefore required when convoluting the solar spectrum at TOA (which increases over the 280-400 nm spectral interval), the Rayleigh scattering (which decreases over the interval), the ozone absorption (which decreases over the interval), and the cloud and aerosol absorption and scattering parameters, to get inputs for the computation of fluxes over wider spectral intervals, e.g., 5 nm, presently the coarser of the spectral resolutions for the calculations in the UV processor.

Both the Sun's spectrum and the Rayleigh optical thickness are available from theoretical calculations with a high resolution ( $1 \text{ cm}^{-1}$ ) (Kurucz, 1992; Fontenla et al, 1999; Bodhaine et al., 1999). The spectroscopic parameters of ozone have been known from spectroscopic measurements with resolution from 5 nm (Paur and Bass, 1985; Molina and Molina, 1986) to 0.15 nm (Bogumil et al., 2000). On the other hand, optical parameters for liquid and ice water clouds (absorption coefficient, single scattering albedo, asymmetry factor) are only defined at a limited number (4) of wavelengths in the 280 to 400 nm range (Slingo, 1989; Fu, 1996). It is generally thought that the cloud optical properties vary little over the UV part of the spectrum (Kylling et al., 1997; Josefsson and Landelius, 2000) and that most of the spectral variation in the surface UV flux is linked to the spectral variations in Rayleigh scattering and  $O_3$  absorption. A similar situation prevails for tropospheric aerosols with optical parameters only available at 4 wavelengths, for example, in Hess et al. (1998).

Figure 1 presents the incident solar radiation at the top of the atmosphere with the corresponding input data (at 0.2, 1 and 5 nm resolution) used in the UV processor. The ozone absorption coefficient from Molina and Molina (1986) and the derived absorption coefficients used in the parametrisation are shown in Figure 2a, whereas that for Rayleigh scattering is presented in Figure 2b.

In the last ten years, attention has particularly been focused at the impact of clouds on the UV radiation at the surface (Bordewijk et al, 1995; Bodeker and McKensie, 1996; Kylling et al., 1997; Erlick et al., 1998; Matthijsen and Tanner, 1998; Mayer et al., 1998; Josefsson and Landelius, 2000; Matthijsen et al., 2000; Krotkov et al., 2001). Over the UV part of the spectrum, scattering is generally conservative (no absorption), and it is generally thought that the cloud optical properties vary little so that most of the spectral variation in the surface UV flux is linked to the spectral variations in Rayleigh scattering and  $O_3$  absorption. As a result, these variations, through the multiple scattering between clouds and surface, make the cloud impact on the UV flux at the surface more wavelength-dependent than would be inferred from the small variations in intrinsic cloud optical properties.

Finally, if the spectral UV reflectivity of snow-covered surfaces has received attention over the last 25 years (Wiscombe and Warren, 1980; Warren and Wiscombe, 1980; Warren, 1982; Eck et al, 1987; Grenfell et al., 1994; Schwander et al., 1999; Kylling et al., 2000; Arola et al., 2003) due to the apparition of ozone holes and the increased potential impact on human health, there are still major uncertainties on how large the spatial radius must be when trying to derive a surface albedo in the UV over a particular geographical point surrounded by patchy snow, due to the large contribution of multiple scattering on the downward flux at the surface (Deguener et al., 1998). Also, relatively few attempts have been made at building climatology of surface albedo in the UV-B and UV-A bands in absence of snow (Blumthaler and Ambach, 1988; Herman and Celarier, 1997), as the albedo is much smaller (0.10 over the ocean, < 0.05 over vegetated land). The UV surface albedo has been studied locally from aircraft measurements (Webb et al., 2000), but there appears to be only very few global distributions of the surface albedo from satellite observations. Eck et al. (1987) derived such a distribution at 370 nm from TOMS (Total Ozone Mapping Spectrometer) on board Nimbus 7. Herman and Celarier (1997) reprocessed 14.5 years of the same data and produced a climatology of the 340-380 nm surface albedo. More effort has been aimed at retrieving directly the UV irradiance at the surface from satellite observations (Bodeker and McKensie, 1996; Krotkov et al., 1998, 2001; Kalliskota et al., 2000).

Although a surface with low albedo displays a smaller contribution to multiple scattering and less impact on the UV flux, the usual decrease of albedo between visible and UV regions (shown for a number of natural surfaces in Figure 3, from Feister and Grewe, 1995), if not properly accounted for in calculations, can introduce small but systematic errors, similar to errors introduced by uncertainties on the characterisation of aerosols or the optical properties of clouds (see section 3a). In the past, schemes diagnosing parameters from NWP outputs have usually used a fixed surface albedo (0.02 for BMRC; 0.05 for US NWS). In this respect, it must be noted that the ECMWF model surface albedo, even the more recent one derived from MODIS observations (not yet operational in the IFS), does not represent this decrease in surface albedo from visible to UV. Moreover, the diagnostic of the UV radiation flux into the surface might be of interest to other communities (oceanography, soil science).

### *b. The RT scheme*

The downward fluxes at the surface in either 0.2, 1 or 5 nm wide spectral intervals are computed with a scheme similar to the operational ECMWF SWRT scheme (Morcrette, 1991; Morcrette, 2002). Details are given in the Appendix. Its inputs are the distribution of temperature, ozone, cloud fraction and cloud liquid and ice water over 60 vertical levels between the surface and 0.1 hPa, the surface pressure and the surface albedo. Cloud optical parameters are derived from Slingo (1989) for liquid water clouds and from Fu (1996) for ice water clouds. Mixed clouds are diagnosed from temperature following Matveev (1984). Effective radius of liquid water clouds are diagnosed using Martin et al. (1992), and effective particle size for ice water clouds can be diagnosed from Ou and Liou (1995) or Sun (2001). Extinction coefficient, single scattering albedo and asymmetry factor for continental, maritime, desert and urban aerosols are derived from Hess et al. (1998), and their geographical distributions are taken from the monthly climatology of Tegen et al. (1997). Background stratospheric aerosols are uniformly distributed on the horizontal and have their optical properties from Tanré et al. (1984). In the ECMWF IFS, the snow-free land surface albedo is interpolated from the monthly mean values of a snow-free albedo produced for the combined 1982-1990 years (Los et al., 2000) using the method of Sellers et al. (1996). The surface albedo in the UV-A and UV-B is assumed to be 0.75 and 0.5 times the visible albedo for snow-free land. The factors are 0.95 and 0.9 respectively for UV-A and UV-B over snow-covered land. Over the ocean, the UV albedo is set at 10 percent.

For each of the 600 (at 0.2 nm), 120 (at 1 nm) or 24 (at 5 nm) spectral intervals between 280 and 400 nm, the Sun incident radiation, Rayleigh optical thickness, and optical properties for ozone, clouds and the climatological aerosols (from Tegen et al., 1997; Tompkins et al., 2005) are first derived and used as inputs for the Delta-Eddington method used to compute the fluxes. Outputs are the downward shortwave radiation in the spectral intervals for both clear and total sky conditions.

The UV processor was tested on various datasets. Results of its sensitivity to input parameters are presented in section 3.

### *c. UV-related products*

As stated in the Introduction, the spectral information provided by the high resolution RT codes or the UV processor discussed here is usually not used as such. Usually, the UV irradiance is transformed into, first, a biologically effective dose (BED), then for public distribution into a UV Index. The BED is obtained by convoluting the spectral irradiance at the surface by the erythema action spectrum (Figure 4), the response function of the human skin to UV radiation. The UV Index, an integer, which varies between 1 and more than 15, is then obtained by taking the integer part after multiplying the BED by 40.

### 3. Sensitivity to input parameters.

#### a. Spectral resolution

During its development, the UV processor was first run off-line on a time-series of fields extracted from the ECMWF model over the ARM-SGP site for April and May 1999 (Morcrette, 2002), and using the climatological ozone from Fortuin and Langematz (1994), in order to evaluate how spectral resolution, representation of ozone, cloud properties and surface albedo could impact the surface fluxes.

Table 1 presents for the four spectral resolutions for which the UV processor can be run how various parameters of importance to the computed UV radiation at the surface are conserved when changing the spectral resolution, showing that with the approach used in the development of the processor, the stability of the scheme is very good.

Figure 5 presents, for a clear-sky atmosphere around local noon, the spectral distribution of the downward irradiance at the surface computed by the UV processor and the detailed model UVSPEC (Mayer and Kylling, 2005). As can be seen from the bottom part of Figure 5, the UV processor at 0.2 nm has a level of spectral details similar to the UVSPEC model, very often used for UV studies. Depending on which features of the spectrum are required (e.g., 305, 310, 320, and 380 nm), the UV processor at 1 nm might be a reasonable compromise to represent the spectrum. If a more detailed representation is required, the UV processor could be used at 0.2 nm resolution and could give a good spectral description, while handling the aerosol and cloud processes as in the ECMWF operational scheme, without need for equivalent cloud parameters (e.g., cloud fraction and/or water content or optical thickness averaged over the vertical).

Number of Intervals	Resolution (nm)	Incident Solar Radiation ( $Wm^{-2}$ )	Rayleigh Optical Thickness	Ozone Absorption Coefficient
24	5.	0.1057502799E+03	0.3293000611E-25	0.1293728681E+02
120	1.	0.1057502799E+03	0.3293000611E-25	0.1293728681E+02
600	0.2	0.1057502799E+03	0.3293000611E-25	0.1293728681E+02
3000	0.04	0.1057502799E+03	0.3293000611E-25	0.1293728681E+02

Table 1: Stability of the governing parameters averaged over the 280-400 nm band for different discretisations.

Figure 6 presents, for the same time around local noon but different days, the spectral fluxes for a clear-sky day, a day with a thin high-level cloud, a day with thicker high-level cloudiness, and a day with overcast low-level liquid water cloud. Over these four days in April 1999, the cosine of the solar zenith angle only varies from 0.841 to 0.855. Figure 6 presents the incident radiation at TOA (top panel) and at the surface assuming transparent clouds (bottom left panel). Giving the use of climatological aerosols and ozone, there is very little variability in these two quantities, the main difference only resulting from the different spectral resolution used for the UV processor. Figure 6 also presents the surface fluxes in presence of cloudiness (bottom right), and illustrates how high-level ice clouds have a much smaller impact on the surface UV flux than low-level liquid water clouds. Upper part of Figure 7 presents the corresponding time-series, over the first 10 days of April 1999, of the UV flux incident at TOA and the surface fluxes with the clouds either radiatively active (*TotUV*) or assumed fully transparent (*ClrUV*). Between the three lower spectral resolutions (0.2, 1 and 5 nm), the surface fluxes vary little. Between 0.2 and 1 nm, the differences are smaller than 0.03 percent on the 280-400 nm downward fluxes and 0.09 percent on EDR. Between 0.2 and 5 nm, these differences become 0.2 and 3 percent respectively. In both cases, these differences are systematic with the fluxes at 0.2 nm slightly larger than those at 1nm, themselves slightly larger than those at 5nm, showing that Rayleigh scattering and  $Q$

absorption, even when properly spread out over spectral intervals of different resolution, tend to screen less of the downward UV radiation with increasing resolution.

As can be seen in Table 2, the UV processor gives very stable BED, and its sensitivity to changes in the column amount of  $O_3$  is almost independent of the spectral resolution.

Ozone	0.2	1	5
+50%	0.1231	0.1231	0.1199
+20%	0.1626	0.1624	0.1583
reference	0.2053	0.2051	0.2000
-20%	0.2743	0.2739	0.2676
-50%	0.5001	0.4994	0.4927

Table 2: Changes in biologically effective dose ( $Wm^{-2}$ ) for various spectral resolutions of the UV processor. Calculations are for 19990409 18UTC.

Given the very stable results of the UV processor with resolution, the UV Index would also be very stable. For completeness, the BED and UV Index during the first 10 days of April 1999 over the ARM-SGP site are shown in the lower part of Figure 7.

#### b. Definition of the surface albedo

Results presented in Figs. 6 and 7 were obtained with a surface albedo set to 5 percent. The same simulations were repeated for a surface albedo of 0, 5, and 10 percent. A change from 0 to 5 percent increases clear-sky fluxes by 2 percent (and EDR by 3 percent). A change from 5 to 10 percent induces the same response. These increases are directly linked to increase in the multiple scattering between the surface and the atmosphere above, for those wavelengths with radiative energy reaching the surface (from about 300 nm). The impact then goes decreasing with multiple scattering with increasing wavelength. In cloudy situations, the effect is generally similar to that in clear-sky situations, except for low solar zenith angles for which the increase in absorption appears to reduce and sometimes reverse the change in downward flux. However, for the practical purpose of deriving UV-indices, this effect only appears when the available surface insolation is far below any dose rate of concern.

#### c. Impact of aerosols

Another parameter usually known with some uncertainty is the aerosol optical thickness. Table 3 presents, for the situation discussed in Figure 5, how the BED would vary when the optical thickness at 300 nm of the prevailing continental aerosols over the ARM-SGP site varies from 0 to 2 (corresponding to a variation from 0 to 1 at 550 nm). Compared to the sensitivity to the amount of  $O_3$ , the sensitivity to the amount of aerosols is at least one order of magnitude smaller.

At this stage, the UV-processor only accounts for aerosols using the climatologies present in the ECMWF IFS (Tegen et al., 1997). At the end of the GEMS project, a UV product accounting not only for analysed ozone but also for prognosed aerosols should be available.

*d. Dependence on effective size of cloud particles and cloud optical properties*

Tests were carried out modifying the effective radius for liquid water clouds from the diagnostic formulation of Martin et al. (1992) by a 10  $\mu m$  fixed value. Similarly for ice water clouds, the effective particle size was diagnosed either from temperature only according to Ou and Liou (1995) or from temperature and local ice water content following Sun (2001). The impact was as expected from a change in effective particle size translating into a change in optical thickness. For example, over the ARM-SGP site, Martin’s formulation gives an effective radius generally between 4 and 5  $\mu m$ . A fixed value of 10  $\mu m$  decreases the optical thickness of liquid water clouds by about a factor of two, thus increasing the downward UV flux at the surface. In this respect, the sensitivity of the surface UV flux to changing the diagnostic formulation for the effective particle size was found much more important than the overall weak sensitivity to the definitions of the cloud optical properties. In the UV part of the spectrum, the various formulations for both the liquid and ice cloud optical properties (Slingo, 1989; Hu and Stamnes, 1993; Ebert and Curry, 1992; Fu and Liou, 1993; Fu, 1996) give optical thicknesses within a few percent of each other.

In conclusion of this sensitivity study, it has been shown that the UV flux integrated between 280 and 400 nm or the UV products derived from the corresponding spectrum shows little sensitivity to the spectral resolution used to run the UV processor. As expected, the sensitivity to the presence of clouds and to their optical thickness, to the amount of  $O_3$  is large, and the sensitivity to the amount of aerosols was shown to be relatively small.

	clear	high cloud	low cloud
$\mu_0$	0.8445	0.8413	0.8447
TCC	0.	0.374	0.392
AOT	BED	BED	BED
0	0.2071	0.1284	0.1259
0.05	0.2061	0.1278	0.1253
0.1	0.2051	0.1272	0.1247
0.2	0.2031	0.1259	0.1235
0.5	0.1972	0.1223	0.1199
1.	0.1875	0.1162	0.1141
2.	0.1688	0.1046	0.1028

*Table 3: Changes in biologically effective dose ( $Wm^{-2}$ ) for various aerosol optical thicknesses (AOT). Results are presented for a clear-sky atmosphere, and two atmospheres with either a high-level ice cloud or a low-level water cloud, under similar insolation. Calculations are for a 1nm resolution. Aerosols are of the continental average type of Hess et al. (1998), assumed at a 80 percent relative humidity. The optical thickness is given for 300nm.*

**4. UV Diagnostics on-line in the IFS.**

The UV processor has been included in the IFS since cycle 29R3, and can be run interactively with a 5nm spectral resolution every hour to produce UV diagnostics. Tests were done with the model at  $T_511L60$  to quantify their associated costs. Given that the UV index information is likely to be only relevant for high surface insolation (and to minimize the cost of the experimentation), a filter was introduced so that the UV computations were done only for those model grids for which the cosine of the solar zenith angle is higher than 0.01. Results are presented in Figure 10 over the extended European area ( $72^{\circ}N - 20^{\circ}N, 15^{\circ}W - 50^{\circ}E$ ) and show the BED averaged at the hour closest to local noon, on 21 June 2004 from a 24 hour  $T_511L60$  forecast started at 00UTC. The corresponding cloudiness, processed for diagnostic purposes into low-level ( $\eta > 0.8$ ,

$\eta = p/p_{surf}$ ), mid-level ( $0.45 < \eta < 0.8$ ), high-level cloudiness ( $\eta < 0.45$ ) and total cloudiness is shown in Figure 11. The presence of cloudiness leads to a decrease of the BED, generally of the order of 3 to 10 percent, over most of continental Europe, with a maximum reaching 20 percent over the Baltic states.

Figures 12 and 13 compare the BED at local noon for three dates (19980312, 19991130 and 20011108) computed using either the prognostic ozone or the climatological ozone from Fortuin and Langematz (1994) in the UV calculations. The prognostic ozone clearly have minima over various areas for these dates, and the resulting BEDs is larger (up to 35 percent for 19980312 south west of Ireland, up to 50 percent for the South Atlantic areas) relative to the BED computed from the climatological ozone field.

Figure 14 presents a preliminary comparison of the BED computed from the ECMWF IFS with a similar quantity derived from the Ozone Mapping Instrument over Jokioinen ( $60.80^{\circ}N$ ,  $23.30^{\circ}E$ ) and Thessaloniki ( $40.63^{\circ}N$ ,  $22.95^{\circ}E$ ) for the year 2005. While the main signal is obviously related to the annual cycle of insolation, the model-derived quantity provides much of the observed variability. At previously stated, this preliminary product only accounts for aerosols using the climatologies present in the ECMWF IFS (Tegen et al., 1997), which explains in part some systematic errors in clear sky situations, for example for Thessaloniki during the summer months, and the comparison is not done with the exact solar zenith angle (SZA), but with the model SZA within an hour of the observation.

## 5. Concluding remarks

This note has presented a radiative scheme to derive the UV radiation at the surface for wavelengths between 280 and 400 nm (UV-B and UV-A bands) with a resolution of either 0.04, 0.2, 1 or 5 nm. At a 0.04 and 0.2 nm spectral resolution, this scheme is directly competitive with the detailed RT codes (e.g., UVSPEC) used for UV studies, with the advantage of being fully consistent with the treatment of aerosols, and clouds in the rest of the ECMWF IFS.

The scheme is directly related to a shortwave radiation scheme that was prior to June 2007 operational in the ECMWF IFS. Compared to other existing UV RT schemes used to diagnose the UV radiation at the surface (e.g., Mayer, 2005), the scheme discussed in this note provides the full spectral and vertical distribution of the UV irradiances in the 280-400 nm spectral range, with the clouds treated without any approximation additional to those used in the SWRT scheme. Even if a number of features of the full shortwave scheme are absent from this UV scheme (as there is no absorption by  $H_2O$ ,  $CO_2$  or other uniformly mixed gases within the considered spectral interval), this scheme is about 4/20/100 times more expensive than the full shortwave scheme, having 24/120/600 vs. 6 spectral intervals to deal with. Therefore it is not proposed to have this scheme on-line within the IFS during the full length of the operational forecast, but rather to use it

- either over the first 24 or 48 hours with a proper filter on the solar zenith angle to prevent UV computations when the resulting UV Index would likely to be below 2 (roughly when  $\mu_0 \leq 0.2$ ),
- or within a parallel run of the forecast model, but at a lower horizontal resolution,
- or as a post-processor run off-line on the archived fields, for example on a number of relevant grid points corresponding to cities or for which operational UV measurements could be available as part of the UV monitoring network.

At the end of the GEMS project, a UV product accounting not only for analysed ozone but also for prognosed aerosols should become available.

## Acknowledgements

A. Hollingsworth, M. Miller and A. Beljaars are thanked for their comments on the manuscript.

## References

- Arola, A., J. Kaurola, L. Koskinen, A. Tanskanen, T. Tikkanen, P. Taalas, J.R. Herman, N. Krotkov, and V. Fioletov, 2003: A new approach to estimating the albedo for snow-covered surfaces in the satellite UV method. *J. Geophys. Res.*, **108D**, 4531, doi:10.1029/2003JD003492.
- Blumthaler, M., and W. Ambach, 1988: Solar UVB albedo of various surfaces. *Photochem. Photobiol.*, **48**, 85-88.
- Bodeker, G.E., and R.L. McKenzie, 1996: An Algorithm for Inferring Surface UV Irradiance Including Cloud Effects *J. Applied Meteor.*, **35**, 1860-1877.
- Bodhaine, B.A., N.B. Wood, E.G. Dutton, and J.R. Slusser, 1999: On Rayleigh optical depth calculations. *J. Atmos. Ocean. Technol.*, **16**, 1854-1861.
- Bogumil, K., J. Orphal, and J.P. Burrows, 2000: O<sub>3</sub> absorption cross-sections at 203, 223, 243, 273 and 293 K. Report, Univ. Bremen, Germany.
- Bordewijk, J. A., H. Slaper, H. A. J. M. Reinen, E. Schlamann, 1995: Total solar radiation and the influence of clouds and aerosols on the biologically effective UV, *Geophys. Res. Lett.*, **22**, 2151-2154, 10.1029/95GL01506.
- Burrows, W.R., M. Vallee, D.I. Wardle, J.B. Kerr, L.J. Wilson, and D.W. Tarasick, 1994: The Canadian operational procedure for forecasting total ozone and UV radiation. *Met. Apps.*, **1**, 247-265.
- Deguenther, M., R. Meerkotter, A. Albold, and G. Seckmeyer, 1998: Case study on the influence of inhomogeneous surface albedo on UV irradiance. *Geophys. Res. Lett.*, **25**, 3587-3590.
- Ebert, E.E., and J.A. Curry, 1992: A parametrisation of ice cloud optical properties for climate models. *J. Geophys. Res.*, **97D**, 3831-3836.
- Eck, T.F., P.K. Bhartia, P.H. Hwang, and L.L. Stowe, 1987: Reflectivity of Earth's surface and clouds in ultraviolet from satellite observations. *J. Geophys. Res.*, **92D**, 4287-4296.
- Erlick, C., J. E. Frederick, V. K. Saxena, B. N. Wenny, 1998: Atmospheric transmission in the ultraviolet and visible: Aerosols in cloudy atmospheres, *J. Geophys. Res.*, **103D**, 31541-31556, 10.1029/1998JD200053.
- Feister, U., and R. Grewe, 1995: Spectral albedo measurements in the UV and visible region over different types of surfaces. *Photochem. Photobiol.*, **62**, 736-744.
- Fontenla, J., O. R. White, P. A. Fox, E. H. Avertt, R. L. Kurucz, 1999: Calculation of solar irradiances. I. Synthesis of the solar spectrum, *Astrophys. J.*, **518**, 480-500.
- Fortuin, J. P. F. and U., Langematz, 1994: *An update on the global ozone climatology and on concurrent ozone and temperature trends*. Proceedings SPIE **2311**, Atmospheric Sensing and Modeling, 207-216.
- Fouquart, Y., and B. Bonnel, 1980: Computations of solar heating of the earth's atmosphere: a new parameterization. *Beitr. Phys. Atmosph.*, **53**, 35-62.
- Fu, Q., 1996: An accurate parameterization of the solar radiative properties of cirrus clouds for climate studies. *J. Climate*, **9**, 2058-2082.

- Fu, Q., and K.-N. Liou, 1993: Parameterization of the radiative properties of cirrus clouds. *J. Atmos. Sci.*, **50**, 2008-2025.
- Grant, W.B., C.F. Garland, and M.F. Hollick, 2005: Comparisons of estimated economic burdens due to insufficient solar ultraviolet irradiance and vitamin D, and excess solar UV irradiance for the United States. *Photochem. Photobiol.*, submitted.
- Grenfell, T. C., S. G. Warren, P. C. Mullen, 1994: Reflection of solar radiation by the Antarctic snow surface at ultraviolet, visible, and near-infrared wavelengths, *J. Geophys. Res.*, **99D**, 18669-18684, 10.1029/94JD01484.
- Herman, J.R., and E.A. Celarier, 1997: Earth surface reflectivity climatology at 340 nm to 380 nm from TOMS data. *J. Geophys. Res.*, **102D**, 28003-28011.
- Hess, P. Koepke, and I. Schult, 1998: Optical properties of aerosols and clouds: The software package OPAC. *Bull. Amer. Meteor. Soc.*, **79**, 831-844.
- Hu, Y.X., Stamnes, K., 1993: An accurate parameterization of the radiative properties of water clouds suitable for use in climate models. *J. Climate*, **6**, 728-742.
- Josefsson, W., and T. Landelius, 2000: Effects of clouds on UV irradiance: as estimated from cloud amount, cloud type, precipitation, global radiation, and sunshine duration. *J. Geophys. Res.*, **105D**, 4927-4935.
- Kalliskota, S., J. Kaurola, P. Taalas, J. R. Herman, E. A. Celarier, N. A. Krotkov, 2000: Comparison of daily UV doses estimated from Nimbus 7/TOMS measurements and ground-based spectroradiometric data, *J. Geophys. Res.*, **105D**, 5059-5068, 10.1029/1999JD900926.
- Koepke, P., and 23 co-authors, 1998: Comparison of models used for UV Index calculations. *Photochem. Photobiol.*, **67**, 657-662.
- Krotkov, N. A., P. K. Bhartia, J. R. Herman, V. Fioletov, and J. Kerr, 1998: Satellite estimation of spectral surface UV irradiance in the presence of tropospheric aerosols 1. Cloud-free case, *J. Geophys. Res.*, **103D**, 8779-8794, 10.1029/98JD00233.
- Krotkov, N. A., J. R. Herman, P.K. Bhartia, V. Fioletov, Jand Z. Ahmad, 2001: Satellite estimation of spectral surface UV irradiance 2. Effects of homogeneous clouds and snow. *J. Geophys. Res.*, **106D**, 11743-11760.
- Kurucz, T.L., 1992: *Synthetic infrared spectra*, Infrared Solar Physics, IAU Symp. 154, edited by D.M. Rabin and J.T. Jefferies, Kluwer, Acad., Norwell Massachusetts.
- Kylling, A., A. Albold, G. Seckmeyer, 1997: Transmittance of a cloud is wavelength-dependent in the UV-range: Physical interpretation, *Geophys. Res. Lett.*, **24**, 397-400, 10.1029/97GL00111.
- Kylling, A., T. Persen, B. Mayer, T. Svenoe, 2000: Determination of an effective spectral surface albedo from ground-based global and direct UV irradiance measurements, *J. Geophys. Res.*, **105D**, 4949-4960, 10.1029/1999JD900304.
- Landelius, T., W. Josefsson, 2000: Methods for cosine correction of broadband UV data and their effect on the relation between UV irradiance and cloudiness, *J. Geophys. Res.*, **105D**, 4795-4802, 10.1029/1999JD900982.
- Lemus-Deschamps, L., L.J. Rikus, 1999: The operational Australian ultraviolet index forecast. *Met. Apps.*, **6**, 241-251.
- Long, C.S., 2003: UV Index forecasting practices around the world. WCRP/SPARC Newsletter 21. <http://>
- Long, C.S., A.J. Miller, H.-T. Lee, J.D. Wild, R.C. Przywarty, and D. Hufford, 1996: Ultraviolet index forecasts issued by the National Weather Service. *Bull. Am. Met. Soc.*, **77** 729-748.

- Los, S.O., G.J. Collatz, P.J. Sellers, C.M. Malmström, N.H. Pollack, R.S. deFries, L. Bounoua, M.T. Parris, C.J. Tucker, and D.A. Dazlich, 2000: A global 9-year biophysical land surface dataset from NOAA AVHRR data. *J. Hydrometeor.*, **1**, 183-199.
- Martin, G.M., D.W. Johnson, and A. Spice, 1994: The measurement and parameterization of effective radius of droplets in warm stratocumulus. *J. Atmos. Sci.*, **51**, 1823-1842.
- Matthijssen, J.III, D. J. Tanner, 1998: Photodissociation and UV radiative transfer in a cloudy atmosphere: Modeling and measurements, *J. Geophys. Res.*, **103D**, 16665-16676, 10.1029/97JD02989.
- Matthijssen, J., H. Slaper, H. A. J. M. Reinen, G. J. M. Velders, 2000: Reduction of solar UV by clouds: A comparison between satellite-derived cloud effects and ground-based radiation measurements, *J. Geophys. Res.*, **105D**, 5069-5080, 10.1029/1999JD900937.
- Matveev, Yu. L., 1984 : *Cloud dynamics*. D. Reidel Publishing Co., Dordrecht, 340 pp.
- Mayer, B., 2005: A UV radiation parameterization for the ECHAM4 GCM. *Atmos. Chem. Phys.*, submitted.
- Mayer, B., and A. Kylling, 2005: Technical Note: The **libRadtran** software package for radiative transfer calculations: Description and examples of use. *Atmos. Chem. Phys. Discuss.*, **5**, 1319-1381.
- Mayer, B., A. Kylling, S. Madronich, and G. Seckmeyer, 1998: Enhanced absorption of UV radiation due to multiple scattering in clouds: Experimental evidence and theoretical explanation. *J. Geophys. Res.*, **103D**, 31241-31254.
- McKinley, A.F., and B.L. Diffey, 1987: A reference action spectrum for ultraviolet induced erythema in human skin. *CIE Journal*, 17-22.
- Molina, L.T., and M.J. Molina, 1986: Absolute absorption cross section of ozone in the 185- to 350-nm wavelength range. *J. Geophys. Res.*, **91D**, 14501-14508.
- Morcrette, J.-J., 1991: Radiation and cloud radiative properties in the ECMWF operational weather forecast model. *J. Geophys. Res.*, **96D**, 9121-9132.
- Morcrette, J.-J., 2002: Assessment of the ECMWF model cloudiness and surface radiation fields at the ARM-SGP site. *Mon. Wea. Rev.*, **130**, 257-277.
- Morcrette, J.-J., A. Benedetti, O. Boucher, et al., 2005: GEMS-Aerosol at ECMWF, in *Proceedings of the Global Earth System Monitoring*, ECMWF, 5-9 September 2005.
- Ou, S.C., and K.-N. Liou, 1995: Ice microphysics and climatic temperature feedback. *Atmosph. Research*, **35**, 127-138.
- Paur, and Bass, 1985: Quadrennial Ozone Symposium, Halkidiki, Greece
- Rikus, L., 1997: Prediction of UV-B dosage at the surface. *Aust. Met. Mag.*, **46**, 211-222.
- Schwander, H., B. Mayer, A. Ruggaber, A. Albold, G. Seckmeyer, and P. Koepke, 1999: A method to determine snow albedo values in the UV for radiative transfer modelling. *Appl. Opt.*, **38**, 3869-3875.
- Sellers, P.J., S.O. Los, C.J. Tucker, C.O. Justice, D.A. Dazlich, G.J. Collatz, and D.A. Randall, 1996: A revised land surface parameterization (SiB2) fro GCMs. Part II: The generation of global fields of terrestrial biophysical parameters from satellite data. *J. Climate*, **9**, 706-737.
- Slingo, A., 1989: A GCM parameterization for the shortwave radiative properties of water clouds. *J. Atmos. Sci.*, **46**, 1419-1427.

- Sun, Z., 2001: Reply to comments by G.M. McFarquhar on "Parametrization of effective sizes of cirrus-cloud particles and its verification against observations". *Quart. J. Roy. Meteor. Soc.*, **127A**, 267-271.
- Taalas, P., G. T. Amanatidis, A. Heikkila, 2000: European Conference on Atmospheric UV Radiation: Overview. *J. Geophys. Res.*, **105D**, 4777-4786, 10.1029/1999JD901181.
- Tanré, D., J.-F. Geleyn, and J.M. Slingo, 1984: First results of the introduction of an advanced aerosol-radiation interaction in the ECMWF low resolution global model, in *Aerosols and their Climatic Effects*, H.E. Gerber and A. Deepak, eds., A. Deepak Publishing, Hampton, Va, USA, 133-177.
- Tegen, I, P. Hoorig, M. Chin, I. Fung, D. Jacob, and J. Penner, 1997: Contribution of different aerosol species to the global aerosol extinction optical thickness: Estimates from model results. *J. Geophys. Res.*, **102**, 23,895-23,915.
- Tompkins A. M., C. Cardinali, J.-J. Morcrette, M. Rodwell, 2005: Influence of aerosol climatology on forecasts of the African Easterly Jet, *Geophys. Res. Lett.*, **32**, L10801, doi:10.1029/2004GL022189.
- Warren, S.G., 1982: Optical properties of snow. *Rev. Geophys. Space Phys.*, **20**, 67-89.
- Warren, S.G., and W.J. Wiscombe, 1980: A model for the spectral albedo of snow: I: Pure snow. *J. Atmos. Sci.*, **37**, 2712-2733.
- Webb, A. R., I. M. Stromberg, H. Li, L. M. Bartlett, 2000: Airborne spectral measurements of surface reflectivity at ultraviolet and visible wavelengths. *J. Geophys. Res.*, **105D**, 4945-4948, 10.1029/1999JD900813.
- Wiscombe, W.J., and S.G. Warren, 1980: A model for the spectral albedo of snow: II: Snow containing atmospheric aerosols. *J. Atmos. Sci.*, **37**, 2734-2745.
- WMO, 1997: Report on the WMO-WHO meeting of experts on standardization of UV Indices and their dissemination to the public. *WMO GAW*, **127**.

## List of Figures

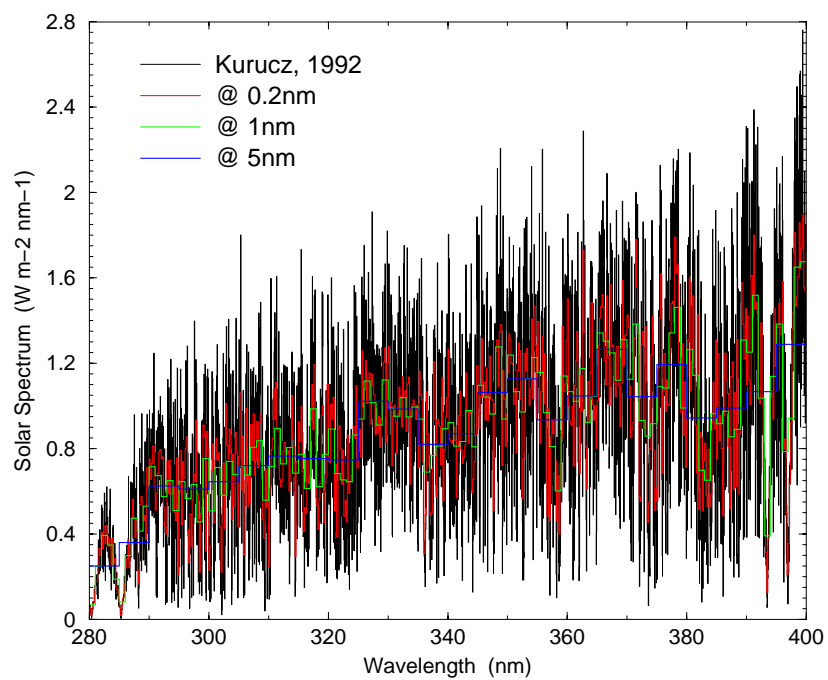


FIG. 1. The incident solar radiation at the top of the atmosphere from Kurucz (1992) and the corresponding input data at 0.2, 1 and 5 nm resolution, for the UV processor.

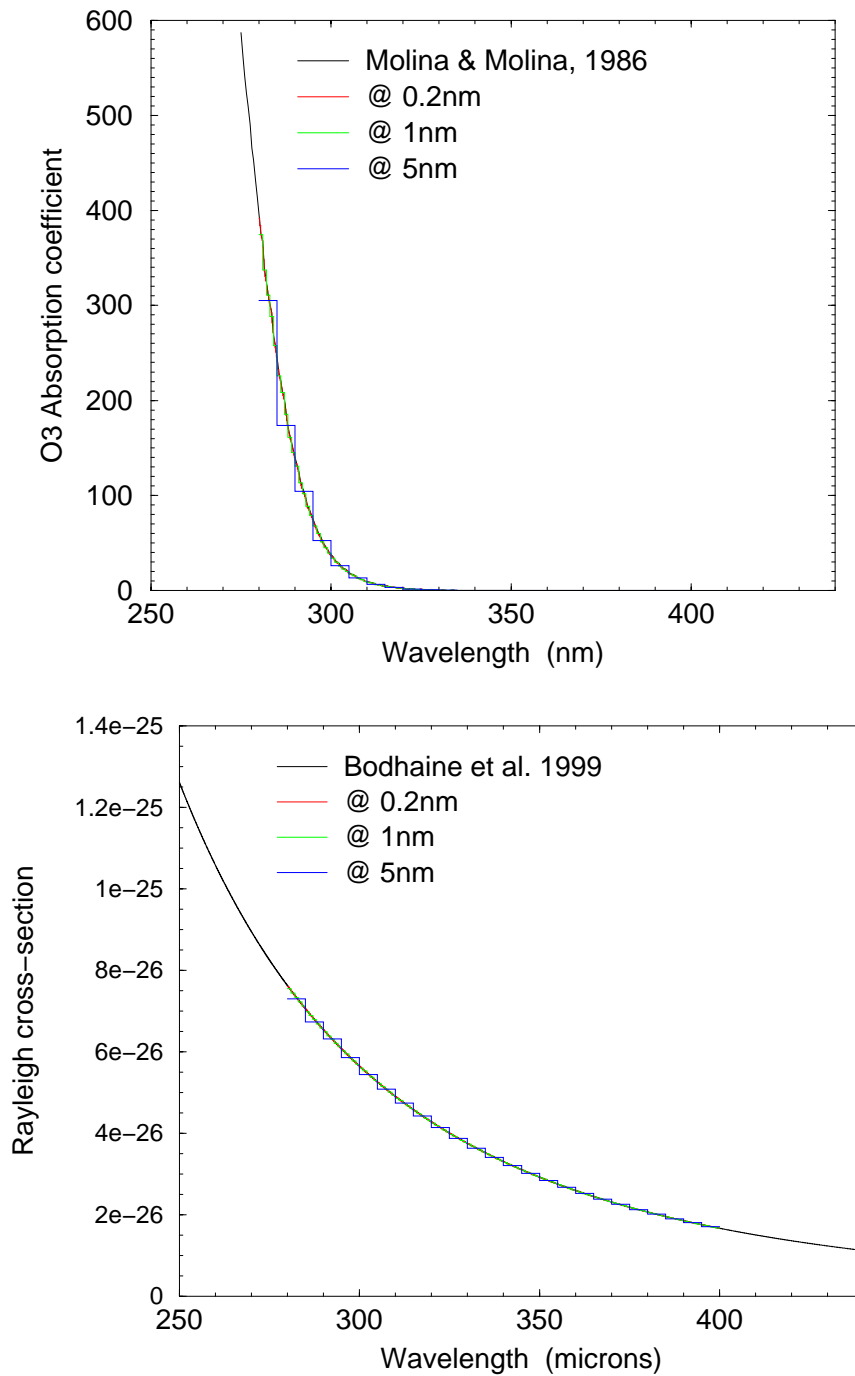


FIG. 2. Upper panel: The ozone absorption coefficient from Molina and Molina (1986) and the corresponding input data at 1 and 5 nm resolution for the UV processor. Lower panel: The Rayleigh cross-section from Bodhaine et al. (1999) and the corresponding input data at 1 and 5 nm resolution for the UV processor.

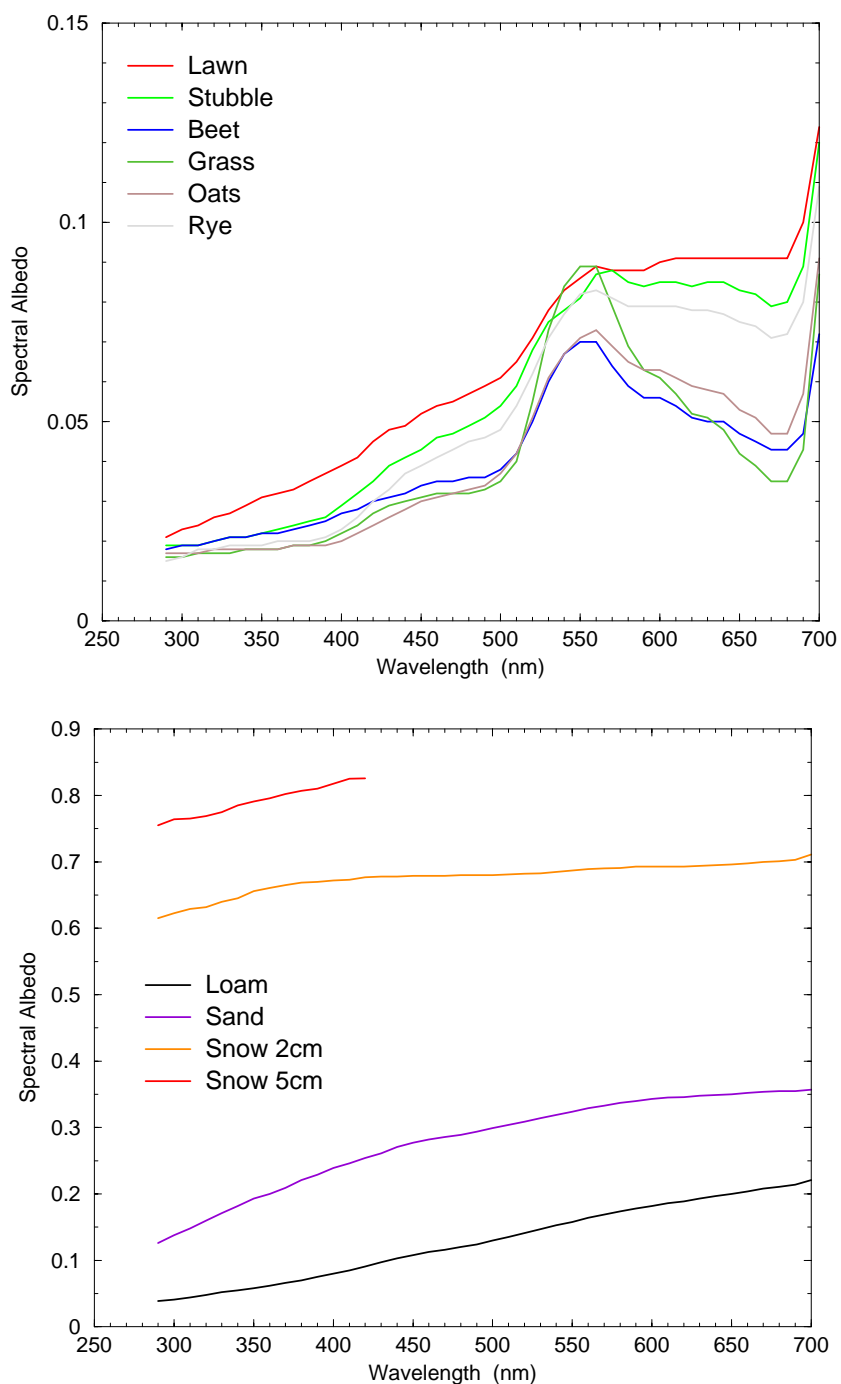


FIG. 3. Upper panel is the spectral albedo over different vegetation surfaces from Feister and Grewe (1995). Lower panel is the spectral albedo over loam, sand, and a 2- and 5-cm thick snow layer, from Feister and Grewe (1995).

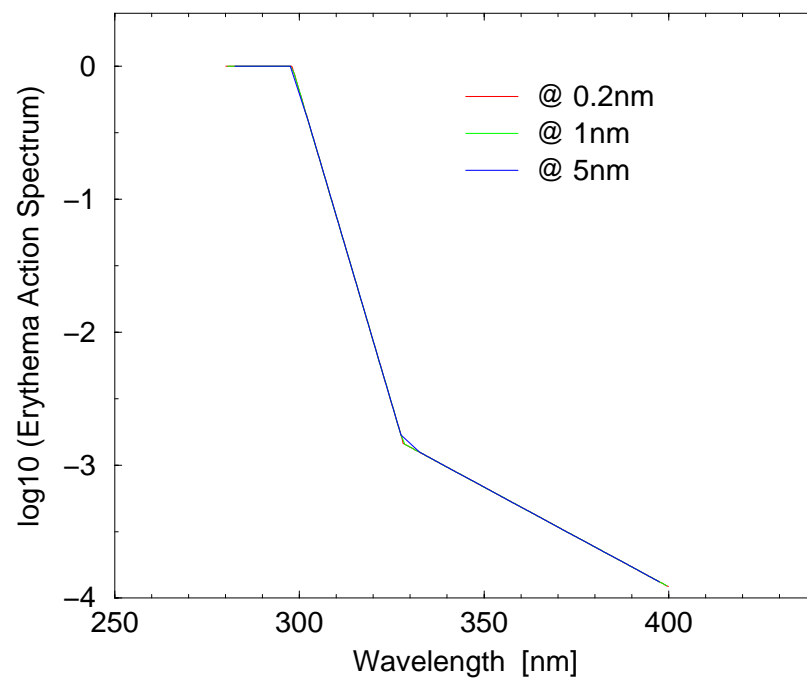


FIG. 4. The Erythema Action Spectrum of McKinley and Diffey (1987), used to derive biologically effective dose (BED).

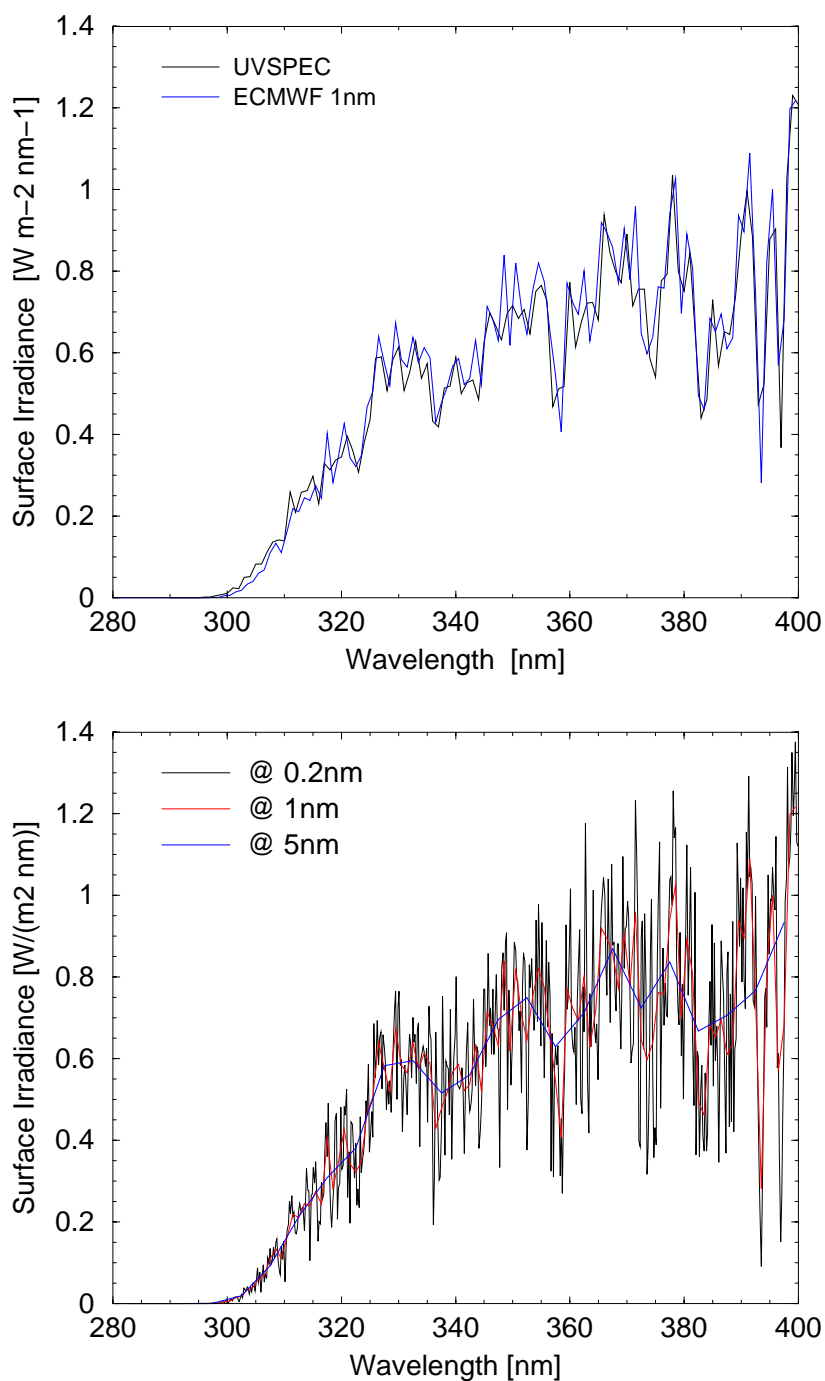


FIG. 5. The spectral radiation at surface for a clear-sky situation over the ARM-SGP site: Upper panel compares the result of the UV processor at 1nm with a computation with the detailed UVSPEC model. Lower panel presents the results of the UV processor at 0.2, 1 and 5 nm for the same situation. Computations are for 19990409 18UTC, with the cosine of the solar zenith angle  $\mu_0 = 0.8713$ .

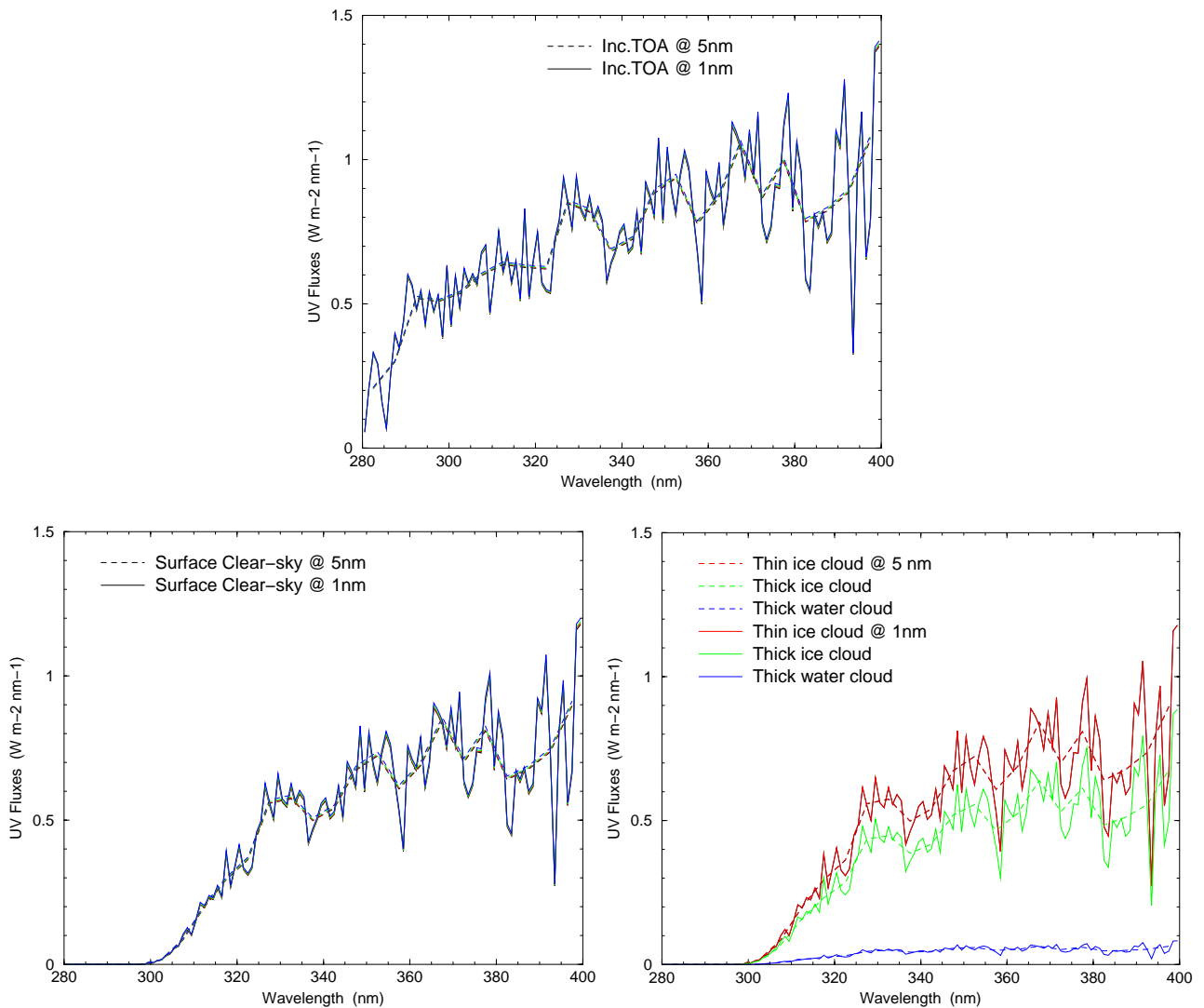


FIG. 6. The spectral radiation at TOA and surface for 4 situations over the ARM-SGP site: Upper panel is the top of the atmosphere incident radiation; Lower left panel is the surface radiation assuming transparent clouds; lower right panel is the surface radiation for thin high-level ice cloudiness, thick high-level ice cloudiness, and thick low-level liquid water cloudiness. Results are shown for both 5 and 1 nm spectral resolutions. All situations at the same local time on 4 consecutive days between 19990401 and 19990405, with  $\mu_0$  0.845. See text for details.

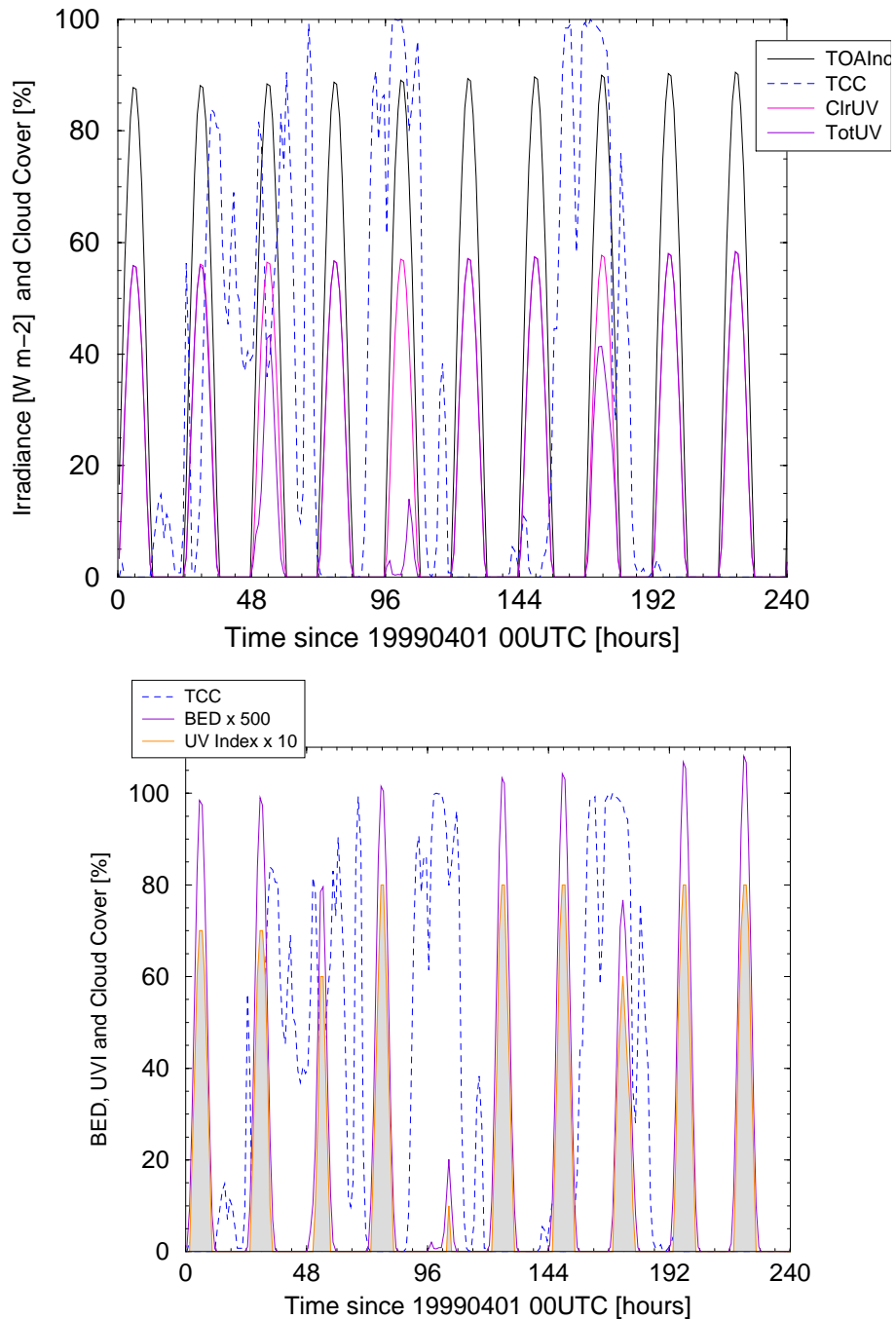


FIG. 7. Upper panel: The surface downward UV radiation over the ARM-SGP site between 19990401 00UTC and 19990410 24UTC. Computations are done with the UV processor at 1 nm. *TOAInc* is the solar radiation incident at the top of the atmosphere in the 280-400 nm range. *TCC* is the total cloud cover within the UV processor, *ClrSky* and *TotSky* respectively refer to the surface irradiance in the same spectral range, assuming clear sky conditions or actual clouds. Lower panel: The corresponding biologically effective dose (BED) corresponding to the 1 nm computations shown above.

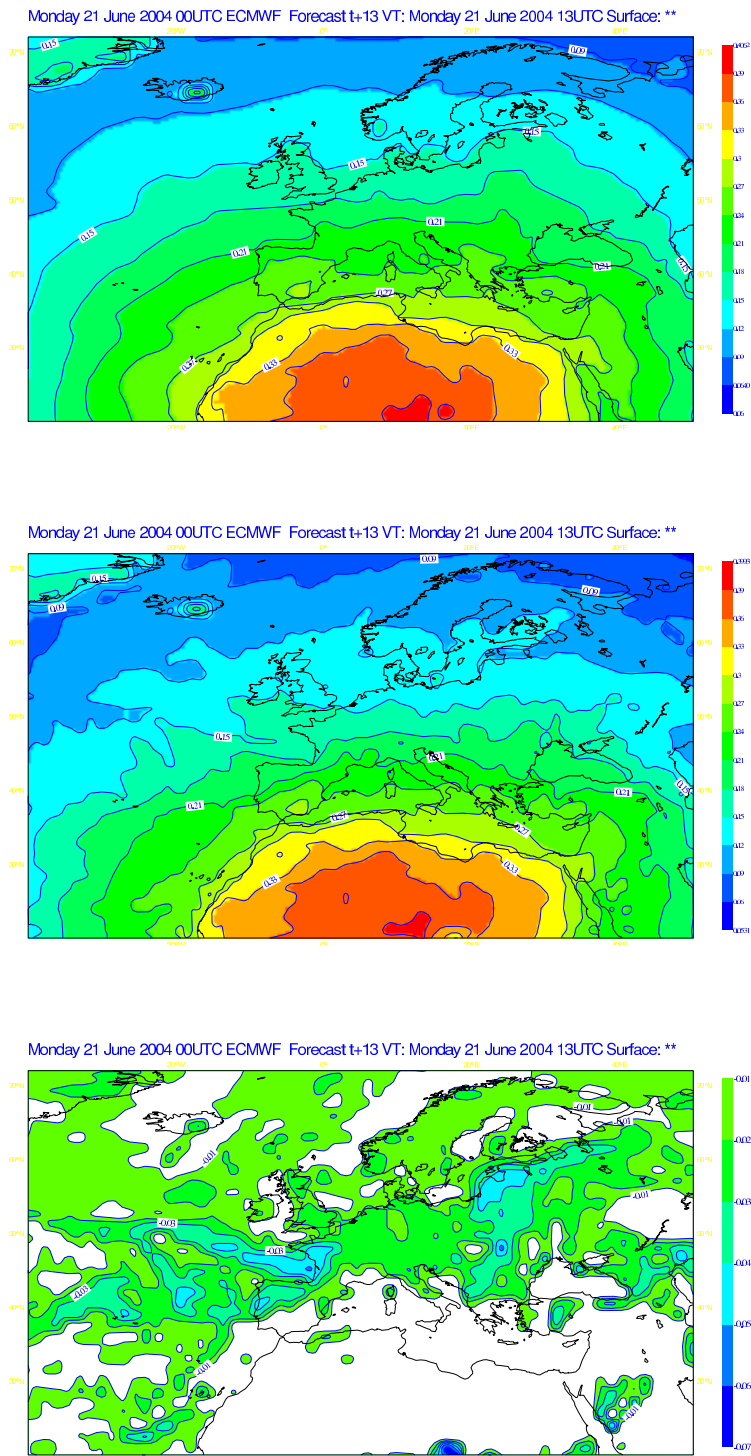


FIG. 8. The biologically effective dose (BED) over Europe on 21 June 2004, averaged over 3 hours around 12UTC, from the UV processor at 5nm resolution, embedded in the IFS at  $T_L511L60$ . Upper panel is for a clear sky atmosphere; middle panel is for the same atmosphere with clouds, with the cloud forcing on the surface BED ( $ClrSky - TotSky$ ) in the lower panel. Scales are  $0.03 Wm^{-2}$  for the BEDs and  $0.004 Wm^{-2}$  for the BED cloud forcing.

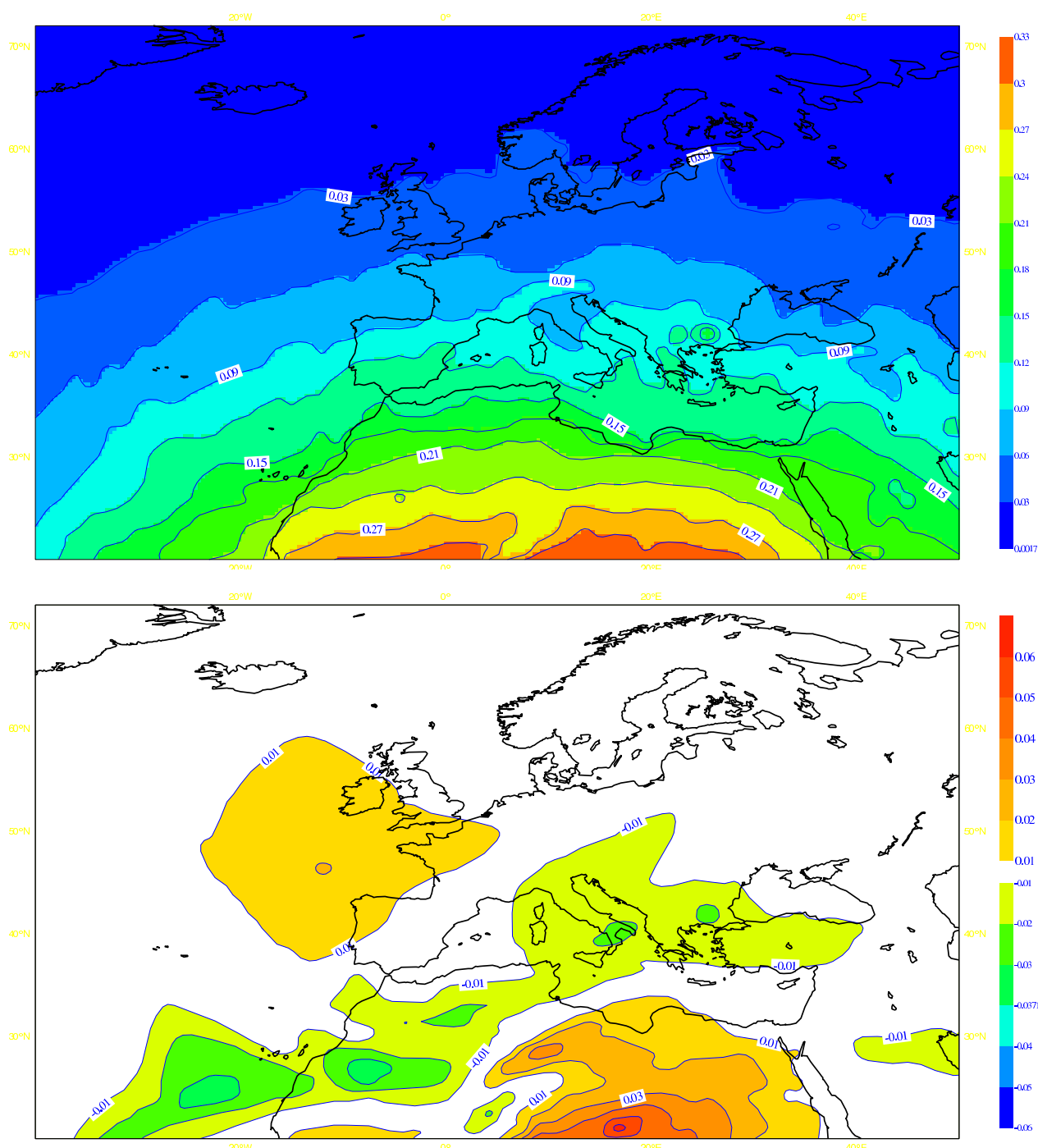


FIG. 9. The BED over the European area computed for noon on 19980312 from ERA40 analyses. Upper panel is the BED using prognostic ozone in the UV computations. Lower panel is the difference in BED between UV computations using prognostic and Fortuin and Langematz (1994) climatological ozone. Contour for BED is every  $0.03 \text{ Wm}^{-2}$ . For the difference in BED, first contour is at 0.01, then every  $0.01 \text{ Wm}^{-2}$ .

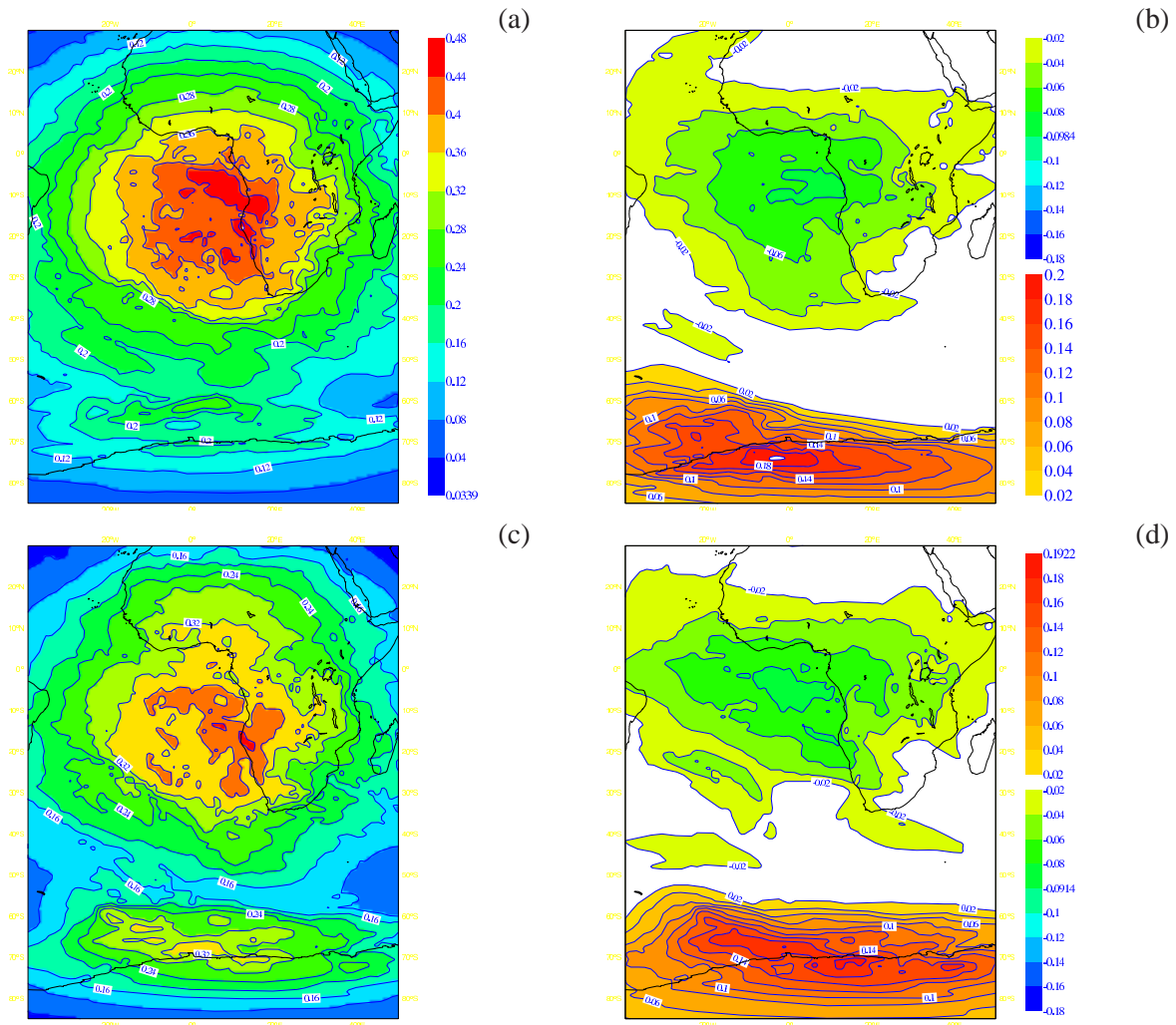


FIG. 10. As in Fig. 12, but for the South Atlantic area. Upper figures are for 19991130, lower figures for 20011108. Contour for BED is every  $0.04 \text{ Wm}^{-2}$ . For the difference in BED, first contour is at 0.02, then every  $0.02 \text{ Wm}^{-2}$ .

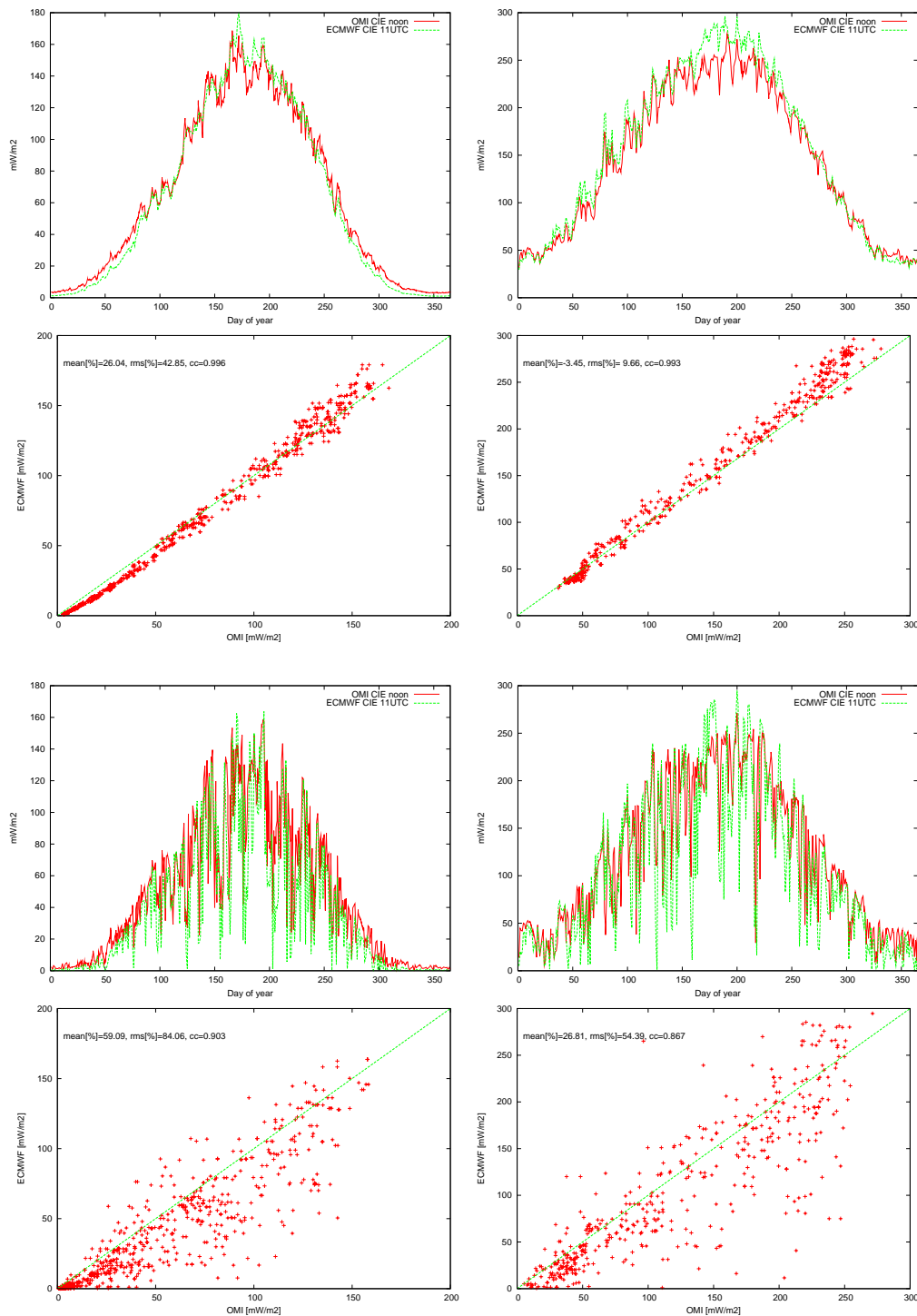


FIG. 11. The biologically effective dose of UV over Jokioinen, Finland (left panels) and Thessaloniki, Greece (right panels), over the year 2005. Results for clear sky situations are in the upper four panels, for total sky in the lower panels. *ECMWF* refers to the UV processor run on-line in  $T_L159L60$  36-hour forecasts started every 24 hours from the ECMWF operational analyses. *OMI* is the equivalent quantity derived from the Ozone Mapping Instrument on-board the Aura satellite.